24th COBEM - 2017

24th ABCM International Congress of Mechanical Engineering
December 3-8, 2017, Curitiba, PR, Brazil

COBEM-2017-0900
A CASE STUDY OF A LQG/LTR CONTROLLER APPLIED TO UAV: A PRACTICAL APPROACH

Paulo Rogerio Ferreira
Neusa Maria Franco Oliveira
Instituto Tecnológico de Aeronáutica, Departamento de Engenharia Eletrônica e de Computação.
Praça Marechal Eduardo Gomes, 50. Vila das Acácias. São José dos Campos, SP – Brazil
paulorogerio01@gmail.com, *neusa@ita.br*

Abstract. *This paper presents a review of the method of applying an LQG/LTR controller in a mathematical model of a Piper J-3 Cub 1/4 scale aircraft. The method can be used in unmanned aerial vehicle control system design and this review presents the results after applying the methodology in a non-linear model of the aircraft and its corresponding linearized model. A longitudinal control system was simulated and the results demonstrate that the method provides good robustness and performance properties.*

Keywords: *UAV, LQG/LTR, Control System, Non-Linear Model.*

1. INTRODUCTION

Unmanned aerial vehicles, known as UAVs, had its origin mainly in military applications. Despite this, its use has expanded to several areas, such as commercial, scientific, agricultural, surveillance, aerial photography, recreational, etc. The UAVs available in the market use the most diverse platforms of autopilot, commercial and some academic (Abdulhamid, 2016). However, often the process of gain adjustment of the control unit depends on trial and error and a prior knowledge of the system to get the best performance possible. In some cases, a bad choice of the gains can lead to system instability that is potentially catastrophic for unmanned aerial vehicles.

Thanks to advances in processing capacity and technology resources, control system developers have been able to apply more advanced and complex control strategies. The control system of an aircraft must be capable of working, even if there are incompatibilities between the nominal model and the real plant, due, for example, to linearization errors, variation of the operating point of the plant (used in the modeling), dynamics non-modeled, among others. In this sense, an important approach called Linear Quadratic Gaussian / Linear Transfer Recovery (LQG/LTR) has emerged successfully (Doyle and Stein, 1981; Stein and Athans, 1987) and has been applied to a wide class of situations. The stability margins guaranteed by the linear quadratic regulator (LQR) and its counterpart, the Kalman Filter (KF), provide practical solutions to the full-state feedback and state estimation problems. Additionally, the idea of LTR is to recover a Kalman filter loop transfer function. These form the main foundations of the LQG/LTR method.

The longitudinal control of an aircraft must be robust enough to withstand several changes in the aerodynamic behavior of the aircraft. In general, the dynamics of an aircraft are subject to changes in its weight, center of gravity, velocity, external perturbations, among others. Many of these changes can be interpreted as model uncertainties, and in this case, the LQG/LTR methodology becomes a good choice to deal with these uncertainties. A more detailed explanation of the LQG/LTR method can be found in da Cruz (1996) and Athans (1986).

2. DEVELOPMENT

2.1 Aircraft Model

Aircraft are plants with non-linear characteristics but the techniques used to design the LQG/LTR controller use linear and time invariant models, with m inputs, m outputs and n state variables. In this work, a Piper J-3 Cub 1/4 aircraft will be used as an example of application. The mathematical modeling of this aircraft has already been the subject of previous research as presented in Du (2011) and the linearization process was based on the Simplex algorithm (Stevens and Lewis, 2003) that uses iterative optimization methods, thus guaranteeing satisfactory results.

This procedure was performed for the longitudinal dynamics, obtaining an angle of pitch that allows the airplane to fly straight and level.

The aircraft linear model is given in Eq. (1) and its state and input vector in Eq. (2) and (3). The state variables are respectively the aircraft linear velocity on the x-axis (u_b), velocity on the w-axis (w_b), pitch rate (q), pitch angle (θ) and altitude (h). The input variables are respectively the power applied to the engine (δ_T) and elevator deflection (δe).

$$\begin{aligned} \dot{X} &= AX + Bu \\ y &= CX + Du \end{aligned} \tag{1}$$

$$X = \begin{bmatrix} u_b & w_b & q & \theta & h \end{bmatrix}^T \tag{2}$$

$$u = \begin{bmatrix} \delta_T & \delta_e \end{bmatrix}^T \tag{3}$$

Equation (4) presents the matrices of longitudinal linear model in the state space representation.

$$\begin{aligned} A &= \begin{bmatrix} -0{,}1068 & 0{,}4047 & -0{,}7378 & -9{,}8016 & 0{,}0000 \\ -0{,}6310 & -6{,}9080 & 22{,}9883 & -0{,}3147 & -0{,}0009 \\ 0{,}3972 & -12{,}3859 & -26{,}2910 & 0 & -0{,}0000 \\ 0 & 0 & 1{,}0000 & 0 & 0 \\ -0{,}0321 & 0{,}9995 & 0 & -23{,}0000 & 0 \end{bmatrix} \\ B &= \begin{bmatrix} 11{,}6874 & 0 \\ 0 & 0 \\ 0 & -168{,}0094 \\ 0 & 0 \\ 0 & 0 \end{bmatrix} \\ C &= \begin{bmatrix} 0{,}9995 & 0{,}0321 & 0 & 0 & 0 \\ -0{,}0014 & 0{,}0435 & 0 & 0 & 0 \\ 0 & 0 & 1{,}0000 & 0 & 0 \\ 0 & 0 & 0 & 1{,}0000 & 0 \\ 0 & 0 & 0 & 0 & -1{,}0000 \end{bmatrix} \\ D &= \begin{bmatrix} 0 \end{bmatrix}_{5\times 2} \end{aligned} \tag{4}$$

2.2 Modeling of the Parametric Uncertainty

The plant model to be used in the design methodology does not exactly represent the real system, thus a representation for errors and uncertainties must be used.

According to da Cruz (1996) and Athans (1986), in the LQG/LTR method, the representation of the modeling error can be done by the multiplicative error representation shown by Doyle and Stein (1981), where all modeling errors of the plant are reflected in the output. Figure 1 presents the uncertainty model considered in this work.

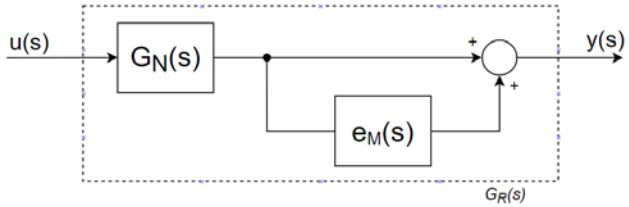

Figure 1. Block diagram of the uncertainty model.

Assuming that $G_R(s)$ represents the real plant dynamics and that the multiplicative error matrix is defined as $E(s)$, reflected at the output of the plant:

$$G_R(s) = \left[I + E(s) \right].G_N(s) \tag{5}$$

Since we do not know the detailed expression $E(s)$, then it is assumed that, in the worst case,

$$\sigma_{max} E(j\omega) \le e_M(\omega) \tag{6}$$

Where, $e_M(\omega)$ is known as the magnitude of the error and σ_{max} is maximum singular value. Here it is assumed that the designer is able to establish an upper limit for the error.

2.3 Project of the LQG/LTR controller

The matrix of transfer functions of the nominal plant $G_N(s)$ will be assumed to be square for simplicity, i.e., a square matrix of dimension $m \times m$. We assume $K(s)$ linear and time invariant, with m inputs and m outputs. The signals named as $r(s)$, $e(s)$, $d(s)$, $y(s)$, and $n(s)$ are, respectively, reference (or command), error, disturbance, output of the plant and noise signals. $K(s)$ is the transfer function of the (LQG/LTR) compensator. Figure 2 presents the multivariable loop, with the controller K(s) to be designed.

The matrix $G_N(s)$ can be written as:

$$G_N(s) = C.\phi(s).B \tag{7}$$

where,

$$\phi(s) = (sI - A)^{-1} \tag{8}$$

It is assumed that the pair [A, B] is controllable and the pair [A, C] is observable.

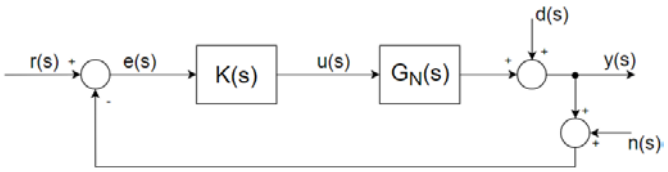

Figure 2. Multivariable feedback loop.

The main purpose of control system design is to provide good closed loop performance and robustness properties. These objectives can be achieved by designing a compensator $K(s)$ as shown in Fig. 2. According to Prakash (1990), the LQG/LTR methodology involves two steps and these can be described as follows:

Step 1: design a structure called Target Feedback Loop (TFL) with a constant gain matrix ("TFL-gain") to meet the performance and robustness requirements at a given point (the "target point") in the loop.

Step 2: design a compensator to recover the properties of the TFL. This compensator has another constant gain matrix ("LTR-gain") and this gain is calculated in such a way that the loop transfer at the target point in the actual closed loop system is approximately equal to the loop transfer of the TFL at the target point. In other words, the system of Fig. 3 approaches point to point of the system represented by Fig. 2.

2.3.1 Target Feedback Loop (TFL)

The structure of the target feedback loop is shown in Fig. 3 and is defined by the parameters C and $\phi(s)$ of the nominal plant and by a constant matrix H ($m \times n$), called the filter gain matrix. If the loop is interrupted at the output, the transfer function matrix $G_{KF}(s)$ associated with the TFL is obtained (Athans, 1986).

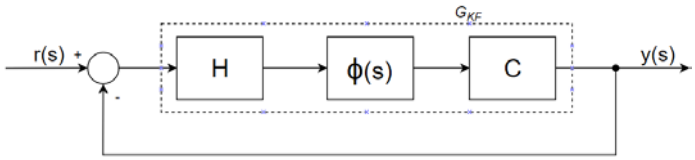

Figure 3. Target Feedback Loop

$$G_{KF}(s) = C.\phi(s).H \tag{9}$$

It is emphasized that the premise that [A, C] is detectable results in the existence of a matrix H that makes the TFL stable. Once the stability of the nominal plant is guaranteed, the inequality given by (10) must be satisfied for the entire frequency range ω to ensure robust stability.

$$\sigma_{\max}\left[I + G_{KF}(j\omega)\right]^{-1}.G_{KF}(j\omega) < \frac{1}{e_M} \tag{10}$$

The Kalman filter (KF) loop has good robustness properties, specifically to perturbations at the output, and further is amenable to output tracking. The filter gain matrix *H* is fixed to be found in the target loop using the KF techniques.

To design the gain matrix *H*, we consider the system written as:

$$\begin{aligned} \dot{x} &= Ax + L\xi \\ y &= Cx + v \end{aligned} \tag{11}$$

where, *L* is a $n \times m$ matrix and, ξ and *v* are white noise processes with zero mean and are independent.

The matrix *H* is found by solving the Riccati Algebraic Equation, given by:

$$0 = -A\Sigma - \Sigma A^T - LL^T + \frac{1}{\mu}\Sigma C^T C\Sigma \tag{12}$$

$$H = \frac{1}{\mu}\Sigma C^T \tag{13}$$

It is observed that the matrix *L* and the scalar parameter μ are design parameters that determine the matrix *H*. Thus, it should be checked whether [*A, L*] is stabilizable and if [*A, C*] is detectable so that the nominal stability of the target feedback loop is guaranteed for any values of μ and *H*. Furthermore, when is necessary to adjust the crossover frequency to meet the conditions of the robustness and stability barriers, one can change μ to a more adequate value.

As reported by da Cruz (1996), the LQG/LTR compensator must be designed in such a way that the steady error is null for constant arbitrary commands (step), which implies the addition of integrators. Beyond that, it is desired that all singular values be equal for low and high frequencies. For this, the solution proposed redefines the system matrices as follows:

$$\begin{aligned} A &= \begin{bmatrix} 0 & 0 \\ A_N & B_N \end{bmatrix} \\ B &= \begin{bmatrix} 1 \\ 0 \end{bmatrix} \\ C &= \begin{bmatrix} 0 & C_N \end{bmatrix} \end{aligned} \tag{14}$$

After increasing the system, da Cruz (1996) defines the matrix *L*, decomposed as:

$$L = \begin{bmatrix} L_L \\ L_H \end{bmatrix} \tag{15}$$

The matrix L_L is used to manipulate the behavior of the singular values at low frequencies and the matrix L_H to manipulate the behavior of the singular values at high frequencies. The matrices L_L and L_H can be calculated in order to obtain the matching of the singular values as follows:

$$L_L = -\left[C.A^{-1}.B\right]^{-1} \tag{16}$$

$$L_H = -\left[A^{-1}.B.L_L\right] \tag{17}$$

After finding the matrix *H* that grants $G_{KF}(s)$ the desired characteristics, one must proceed in the design of the compensator *K(s)* of Fig. 2 such that feedback system behavior approaches the behavior of Fig. 3. Particularly, it is necessary that (18) be satisfied I n the relevant frequency regions to obtain the characteristics desired for the performance.

$$G_N(s).K(s) \approx G_{KF}(s) \tag{18}$$

2.3.2 The LQG/LTR compensator, K(s)

The LQG/LTR compensator has in its structure a replica of the plant dynamics with two feedback loops, one with the filter gain matrix *H* and another with the gain matrix *G*. From the diagram of Fig. 4 we have the expression of *K(s).*

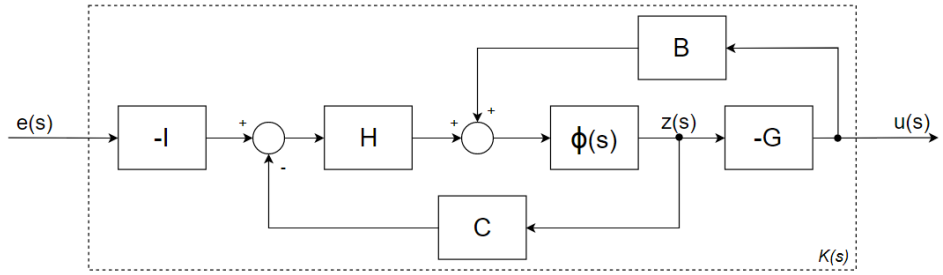

Figure 4. The LQG/LTR compensator, K(s)

$$K(s) = G(sI - A + BG + HC)^{-1} H \tag{19}$$

The control gain matrix *G*, responsible for the recovery of the desired dynamics, is obtained via a solution called the LQR (Linear Quadratic Regulator) problem. It is also calculated by means of the solution of the Riccati algebraic equation as follows:

$$0 = -K_\rho A - A^T K_\rho - C^T C + \frac{1}{\rho} B B^T K_\rho \tag{20}$$

$$G_\rho = \frac{1}{\rho} B^T K_\rho \tag{21}$$

for $\rho \rightarrow 0$.

For the LQR result, if we check the transmission zeros of (7) and conclude that they are all of minimum phase, then for all points we have:

$$\lim_{\rho \to 0} C(sI - A)^{-1} B G_\rho (sI - A + BG_\rho + HC)^{-1} H \rightarrow C(sI - A)^{-1} H \tag{22}$$

that results,

$$\lim_{\rho \to 0} G_N(s) K_\rho(s) \rightarrow G_{KF}(s) \tag{23}$$

Thus, the procedure performs the recovery of the target feedback loop characteristics.

2.4 Design Example

Before applying the design procedure to obtain the LQG/LTR compensator, we must certify the compatibility of linear and nonlinear model. Figure 5 illustrates the case of this example.

From the non-linear model, a longitudinal linear model was extracted with a trim condition that allows flying with level wings.

$$X_{trim} = [u_b \quad w_b \quad q \quad \theta \quad h]^T = [22,9882 \quad 0,7377 \quad 0,0321 \quad 400]^T \tag{24}$$

$$u_{trim} = [\delta_T \quad \delta_e]^T = [0,2398 \quad -0,0544]^T \tag{25}$$

Now, consider the problem of designing a longitudinal attitude control system for an unmanned aircraft. The plant is described by (4) and the state and control vectors are given by (2) and (3). The flight parameters we want to control are the aircraft speed (V_T) and the pitch angle (θ), respectively. Thus, the matrix *C* of the system is reduced to:

$$C = \begin{bmatrix} 0,9995 & 0,0321 & 0 & 0 & 0 \\ 0 & 0 & 0 & 1,0000 & 0 \end{bmatrix} \tag{26}$$

According to Athans (1986), in each system that an LQG/LTR compensator is applied, the greatest effort will be made to specify reasonable performance commitments, to establish the restrictions regarding the robustness of stability and to normalize input and output variables properly. The systematic part of the methodology is generally responsible

for about 10% of the project effort. In order to apply the LQG/LTR control rules in the proposed model, one must define the barriers of stability and performance robustness.

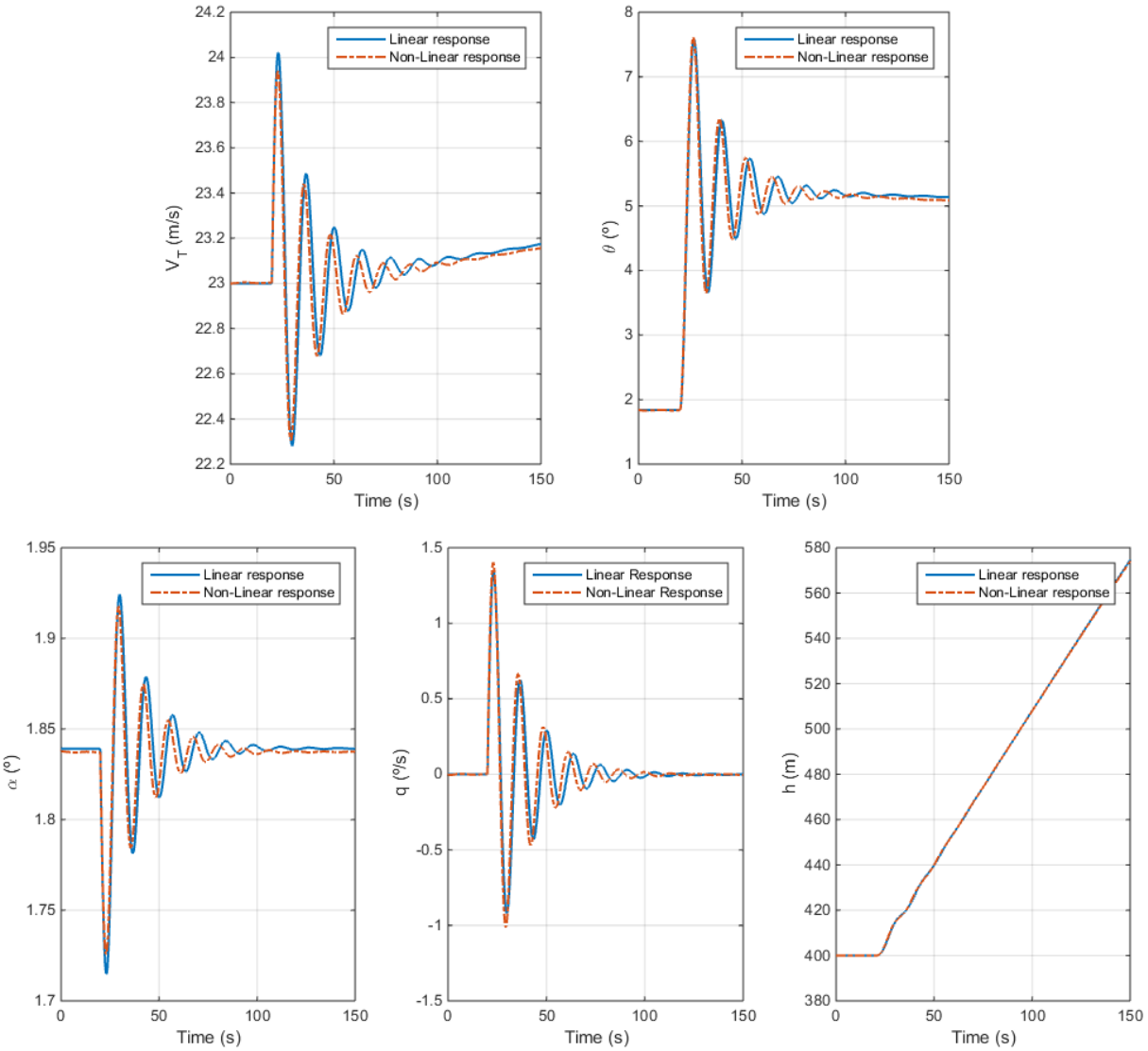

Figure 5. Linear and non-linear responses at the triming condition.

As a result, establishing a compensator that meets the requirements of robustness barriers, allows the controlled system to have the following characteristics: disturbance rejection, tracking of reference signal and insensitivity to plant variations.

Barriers should be established based on the knowledge of the characteristics of the plant and, in this work, the restrictions at low frequencies were defined based on the experience of the process, as presented in Ridgely et al. (1987).

The restrictions are:

- Zero steady state error for step reference input, requiring an integral action on input - increase of the system;
- The system is required to have a gain of at least 20 dB at a frequency of 0,1 rad/s;
- A restriction of 10 rad/s to the maximum cutoff frequency.

For the noise rejection barrier, the frequency ω = 60 rad/s was chosen, from which the system is sensitive to measurement noise.

Regarding the modeling error, we use the modeling error representation described by Stevens and Lewis (2003) which considers only the high frequency limit and assumes that the aircraft model is accurate up to a frequency of 2 rad/s. Then,

$$e_M(j\omega) = \frac{j\omega + 2}{20} \tag{27}$$

In order to satisfy the robustness of stability, the gain of the plant referred to the output must satisfy (10). Thus:

$$\sigma_M\left[G(j\omega)K(j\omega)\right] < \frac{1}{e_M(j\omega)} = \frac{20}{j\omega+2} \tag{28}$$

Figure 6 illustrates the barriers at all frequencies and the singular values, after the addition of integrators, of a Piper J-3 Cub 1/4 scale aircraft.

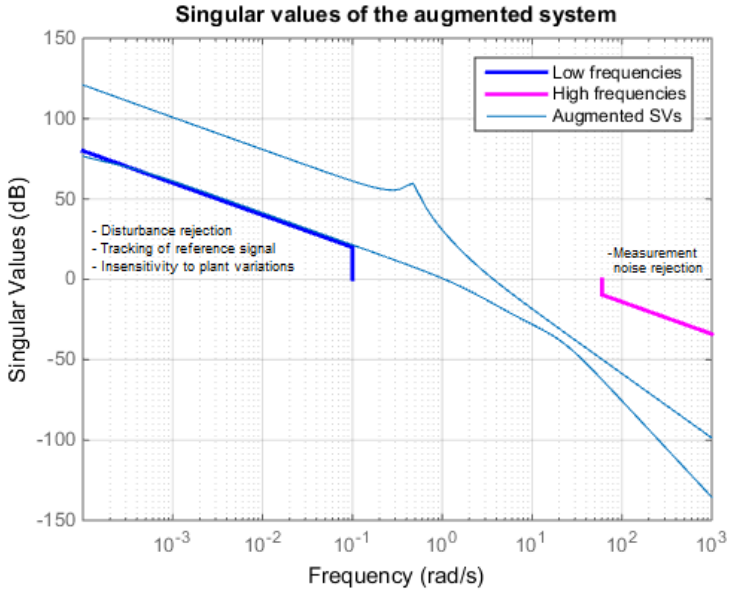

Figure 6. Performance and stability barriers

From this point, the LQG/LTR methodology, as explained in da Cruz (1996), establishes that we should choose μ and L so that the singular values obey the performance and stability barriers. The choice of μ is made by varying its value in order to adjust the desired cutoff frequency and the value of L is chosen in order to obtain a matching in the lows, highs, or in all the frequencies. In this work, we choose a value of μ = 0,05 and the calculation of the matrix L is done by observing (15), (16) and (17). After this, using *Matlab*®, we can solve (12) and calculate the gain matrix H of the Kalman filter given by (13). In a similar way to what was done to find the matrix H, we must find the matrix of gains G solving (20) and (21).

$$L = \begin{bmatrix} 0,0090 & 0,2145 \\ -1,5215.10^{-06} & -1,6961 \\ 0,9995 & -0,7377 \\ 0,0321 & 22,9882 \\ 0 & 0 \\ -1,0588.10^{-22} & 1,0000 \\ -897,6995 & -1,6708.10^{05} \end{bmatrix} \quad H = \begin{bmatrix} 0,0401 & 0,9591 \\ -6,8043.10^{-06} & -7,5853 \\ 4,4698 & -3,2991 \\ 0,1435 & 102,8063 \\ 1,3831.10^{-13} & -9,6367.10^{-14} \\ 3,9413.10^{-14} & 4,4721 \\ -4,0146.10^{03} & -7,4719.10^{05} \end{bmatrix} \quad G = \begin{bmatrix} 34,0281 & 1,1095 \\ 1,1095 & 19,2515 \\ 49,5892 & 0,4534 \\ 2,1128 & 1,0142 \\ -0,3203 & -1,1066 \\ -28,0201 & -50,9484 \\ -6,684.10^{-05} & -6,2167.10^{-05} \end{bmatrix}$$

Finally, we compute the matrix of transfer functions of the compensator given by (19) and find the matrices A_K, B_K, C_K of the compensator, given in state space representation.

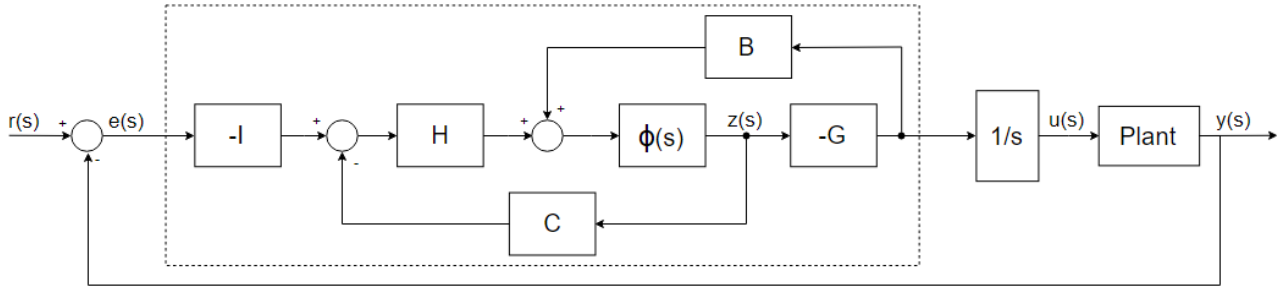

Figure 7. Block diagram of the LQG/LTR compensator with the plant

3. RESULTS AND DISCUSSION

Once the LQG/LTR compensator has been designed, simulations are done applying disturbance and step signals to the closed loop input, in order to verify its responses through different situations. Firstly, the simulations were performed using the linearized plant (longitudinal model) of the aircraft and later the same simulations were performed with the nonlinear plant for comparison. It is important to emphasize and remember that the equilibrium conditions for which this control was designed were given by (24).

In Fig. 8 we see the responses V_T and θ, respectively, after applying on V_T a pulse disturbance of 10% of trim velocity during 0,6 s. The parameter θ was hold without disturbance. It should be noted that in the linear plant, the level zero corresponds to the values of the equilibrium states.

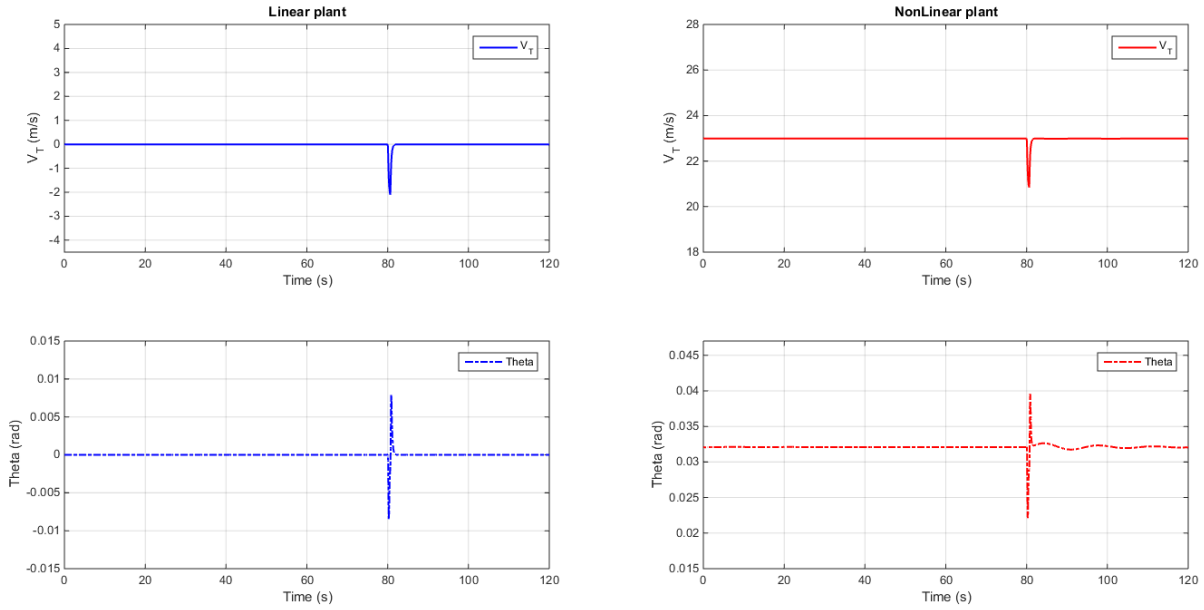

Figure 8. Time response due to disturbance on V_T of linear plant (left) and Time response due to disturbance on V_T of nonlinear plant (right).

In Fig. 9 we also see the response V_T and θ responses, after applying on θ a disturbance of 5º during 0,6 s. The parameter V_T was hold without disturbance.

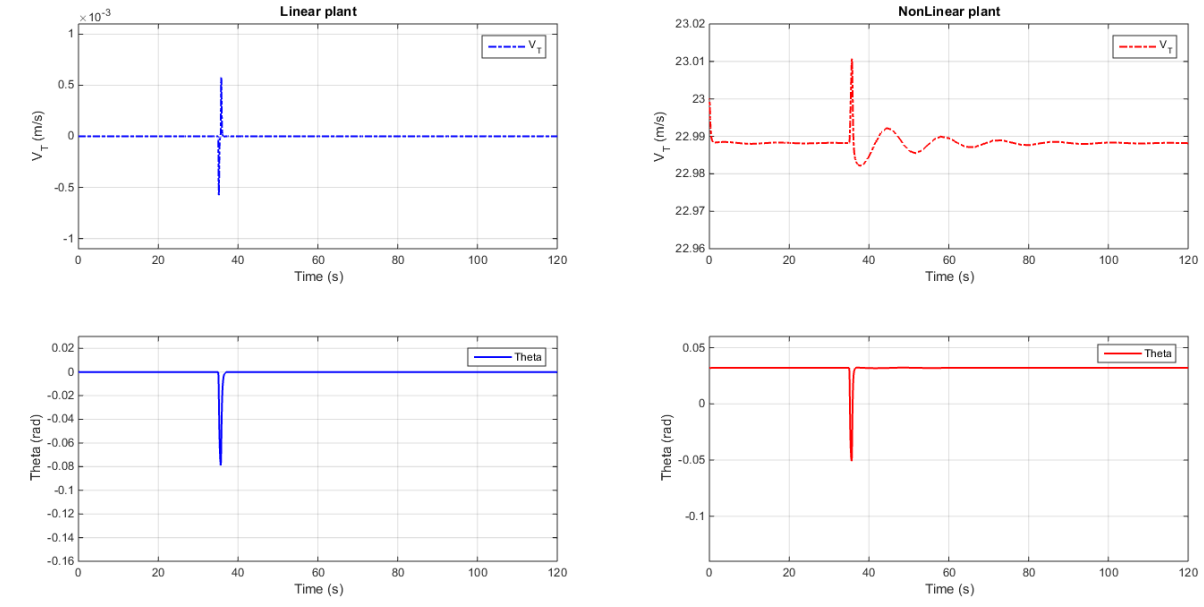

Figure 9. Time response due to disturbance on θ of linear plant (left) and Time response due to disturbance on θ of nonlinear plant (right).

The applied perturbations have characteristics of low and high frequency. However, as observed in Figs. 8 and 9, having applied a disturbance to one parameter, the other was corrected in order to recover the equilibrium conditions. We can further observe that in Fig. 8 there was an overshoot of about 20% on θ due to the disturbance on V_T. However, in Fig. 9 the overshoot on V_T is practically negligible if we consider the order of magnitude.

In Fig. 10 we apply a step of about 13% over V_T. This condition leads the parameters to a region outside the equilibrium states, however, we see the controller acting to track the reference signal and reach equilibrium for this new condition. In this case, we see in the nonlinear plant an overshoot of 0,25% on V_T and, the disturbance response on θ with 38% of overshoot. It was also observed that the main difference between the simulation of linear and nonlinear plants was the oscillation in θ.

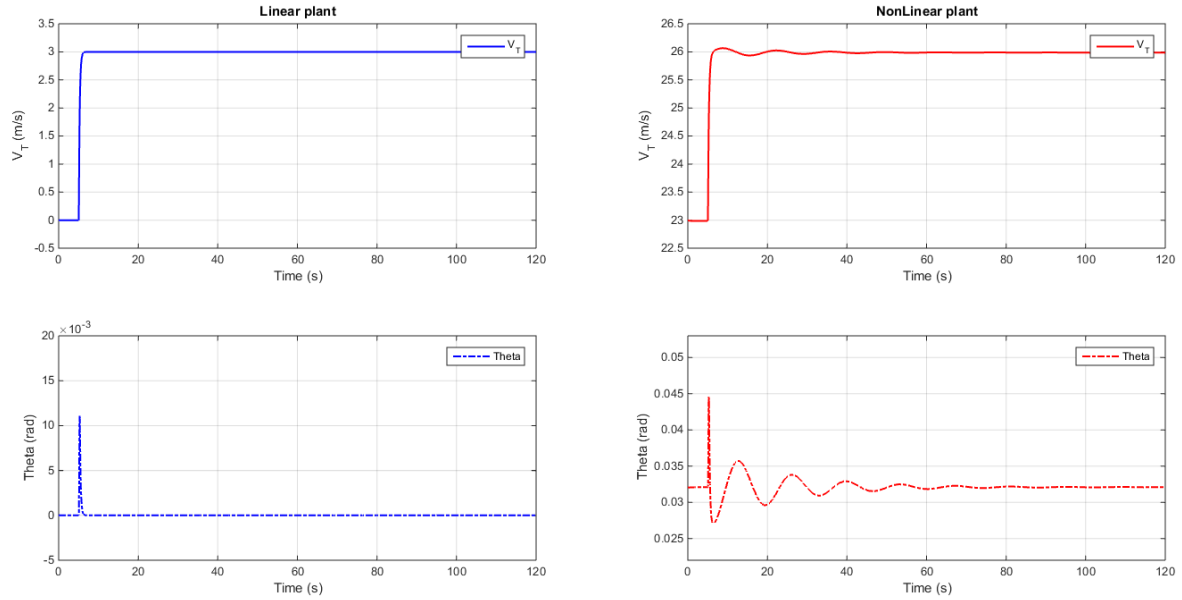

Figure 10. Time response due to step on V_T of linear plant (left) and
Time response due to step on V_T of nonlinear plant (right).

In Fig. 11, we apply an 8º step in θ. Likewise, we notice that a new equilibrium condition is achieved and disturbances caused in V_T are minimal.

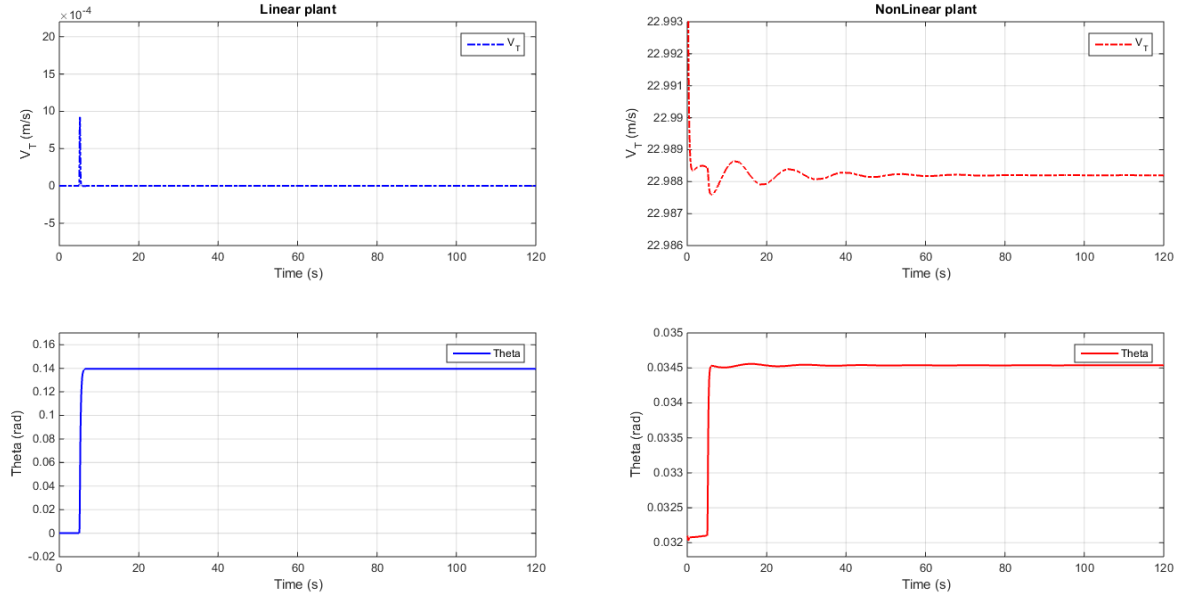

Figure 11. Time response due to step on θ of linear plant (left) and
Time response due to step on θ of nonlinear plant (right).

4. CONCLUSION

This work deals with the systematic study and practical application of the LQG/LTR methodology. The application of this one was satisfactorily carried out and contributed with some considerations about this methodology that has been well studied, but little applied in real situations.

The control used robust methods that were presented in the development. The most complicated step is to design a target feedback loop (TFL) with realistic stability and robustness properties. In the step of calculating the filter gain matrix (H) it is important that the designer has a good knowledge of the concepts about the Kalman filter and the influence of the design parameters μ and the matrix L. Thus, one can meet the requirements of performance and robustness. The simulations evidenced the effectiveness of the control against comparisons in a linear and non-linear system.

5. ACKNOWLEDGEMENTS

The authors acknowledge support provided by CAPES.

6. REFERENCES

Abdulhamid, R., 2016. *Desenvolvimento de Algoritmo de Controle Robusto para Veículos Aéreos Não Tripulados de Asa Fixa de Pequeno Porte*. Dissertation, Instituto Tecnológico de Aeronáutica, São José dos Campos.

Athans, M., 1986. "A Tutorial on the LQG/LTR Method". In *American Control Conference*. Seattle, USA.

da Cruz, J.J., 1996. *Controle robusto multivariável*. Editora da Universidade de São Paulo, São Paulo.

Doyle, J. C. and Stein, G., 1981. "Multivariable feedback design: Concepts for a classical/modern synthesis". *IEEE Transactions on Automatic Control*, Vol. 26, pp. 4-16.

Du, Y., 2011. *Development of real-time flight control system for low-cost vehicle*. Msc by research thesis, Cranfield University, São José dos Campos.

Prakash, R, 1990. "Target feedback loop/loop transfer recovery (TFL/LTR) robust control design procedures". In *29th IEEE Conference on Decision and Control*, Vol. 3, pp. 1203-1209, Honolulu, USA.

Ridgely, D.B. and Banda, S.S. and Mcquade, T.E. and Lynch, P., 1987. "Linear-quadratic-Gaussian with loop-transfer recovery methodology for an unmanned aircraft". *Journal of Guidance, Control, and Dynamics*, Vol. 10, No. 1, pp. 82-89.

Stein, G. and Athans, M., 1987. "The LQG/LTR procedure for multivariable feedback control design". *IEEE Transactions on Automatic Control*, Vol. 32, pp. 105-114.

Stevens, B.L. and Lewis, F.L., 2003. *Aircraft Control and Simulation*. John Wiley & Sons, New Jersey, USA, 2nd edition.

7. RESPONSIBILITY NOTICE

The authors are the only responsible for the printed material included in this paper.